MTOpen

Coformulation of a Novel Human α-Galactosidase A With the Pharmacological Chaperone AT1001 Leads to Improved Substrate Reduction in Fabry Mice

Su Xu[1], Yi Lun[1], Nastry Brignol[1], Rick Hamler[1], Adriane Schilling[1], Michelle Frascella[1], Sean Sullivan[1], Robert E Boyd[1], Kate Chang[1], Rebecca Soska[1], Anadina Garcia[1], Jessie Feng[1], Hidehito Yasukawa[2], Carole Shardlow[3], Alison Churchill[3], Amol Ketkar[4], Nicola Robertson[3], Masahito Miyamoto[2], Kazutoshi Mihara[2], Elfrida R Benjamin[1], David J Lockhart[5], Tohru Hirato[2], Susie Fowles[3], Kenneth J Valenzano[1] and Richie Khanna[1]

[1]Amicus Therapeutics Inc, Cranbury, New Jersey, USA; [2]JCR Pharmaceuticals, Kobe, Hyogo, Japan; [3]GlaxoSmithKline R&D, Ware, Hertfordshire, UK; [4]GlaxoSmithKline R&D, King of Prussia, Pennsylvania, USA; [5]TranscripTx, Inc., San Francisco, California, USA

Fabry disease is an X-linked lysosomal storage disorder caused by mutations in the gene that encodes α-galactosidase A and is characterized by pathological accumulation of globotriaosylceramide and globotriaosylsphingosine. Earlier, the authors demonstrated that oral coadministration of the pharmacological chaperone AT1001 (migalastat HCl; 1-deoxygalactonojirimycin HCl) prior to intravenous administration of enzyme replacement therapy improved the pharmacological properties of the enzyme. In this study, the authors investigated the effects of *coformulating* AT1001 with a proprietary recombinant human α-galactosidase A (ATB100) into a single intravenous formulation. AT1001 increased the physical stability and reduced aggregation of ATB100 at neutral pH *in vitro*, and increased the potency for ATB100-mediated globotriaosylceramide reduction in cultured Fabry fibroblasts. In Fabry mice, AT1001 coformulation increased the total exposure of active enzyme, and increased ATB100 levels in cardiomyocytes, cardiac vascular endothelial cells, renal distal tubular epithelial cells, and glomerular cells, cell types that do not show substantial uptake with enzyme replacement therapy alone. Notably, AT1001 coformulation also leads to greater tissue globotriaosylceramide reduction when compared with ATB100 alone, which was positively correlated with reductions in plasma globotriaosylsphingosine. Collectively, these data indicate that intravenous administration of ATB100 coformulated with AT1001 may provide an improved therapy for Fabry disease and thus warrants further investigation.

INTRODUCTION

Fabry disease is an X-linked lysosomal storage disorder caused by mutations in the gene (*GLA*) that encodes the lysosomal enzyme α-galactosidase A (α-Gal A).[1,2] The primary biological role of α-Gal A is catabolism of neutral glycosphingolipids with terminal α-galactosyl residues, in particular globotriaosylceramide (GL-3, also known as Gb_3 or CTH). Because α-Gal A activity is required for the efficient breakdown of GL-3, reduced enzyme levels result in its accumulation in cells and organs throughout the body, which contributes to the life-threatening manifestations of the disease, such as kidney failure, heart disease, and stroke.[1–3] In addition, the deacylated GL-3 analog globotriaosylsphingosine (lyso-Gb_3), is gaining growing interest. Plasma lyso-Gb_3 is markedly elevated in "classic" male Fabry patients relative to that of normal individuals,[4] with its levels sometimes more than an order of magnitude higher than those of plasma GL-3 (refs. 4–7). In addition, in symptomatic female Fabry patients, plasma lyso-Gb_3 levels tend to be well above normal levels, whereas plasma GL-3 levels tend to be in the normal range.[4–7] Most importantly, elevated plasma lyso-Gb_3 correlates with increased risk of cerebrovascular disease and left ventricular hypertrophy in male and female Fabry patients, respectively, and life-time exposure to plasma lyso-Gb_3 correlates with disease severity.[5]

Enzyme replacement therapy (ERT) is currently the primary treatment for Fabry disease and is based on the intravenous administration of manufactured human α-Gal A, of which Fabrazyme (agalsidase β; Genzyme Corporation, Cambridge, MA) and Replagal (agalsidase α; Shire Pharmaceuticals, Cambridge, MA) are the only two approved products. In some Fabry patients, ERT can reduce GL-3 levels in plasma, urine, and microvascular endothelial cells, alleviate neuropathic pain, reduce hypertrophic cardiomyopathy, increase the ability to sweat, and stabilize kidney function.[8–12] Plasma lyso-Gb_3 levels also are reduced by ERT, which gives some indication of treatment efficacy.[4–7] Although

ERT is effective, the infused enzymes tend to be unstable at neutral pH and body temperature, conditions that mimic the physiological environment during infusion (*i.e.*, the blood), resulting in a short circulating half-life of the properly folded, active enzyme *in vivo*.[8,13] In addition, delivery of ERT to certain cell types, tissues, and organs is insufficient to provide the desired therapeutic effects, as suggested by the inability of infused α-Gal A ERT to significantly reduce GL-3 in cardiomyocytes, distal convoluted tubules, podocytes, and the central nervous system.[8,13] Furthermore, although ERT for Fabry disease is generally well tolerated, the infused enzymes can be immunogenic, which may impair efficacy and negatively affect tolerability.[14–16]

Small molecule pharmacological chaperones (PCs) have been proposed as a potential alternative therapy for Fabry disease.[17] In contrast to ERTs, PCs can be orally available and have broad tissue distribution, including access to the central nervous system.[18] The iminosugar AT1001 (migalastat HCl; 1-deoxygalactonojirimycin HCl) is an analog of the terminal galactose of GL-3 that acts as a selective, reversible, competitive inhibitor of α-Gal A,[19] and can improve the folding, stability, and lysosomal trafficking of multiple endogenous mutant forms of α-Gal A, a subset of which are referred to as "amenable". [17,19–23] Furthermore, AT1001 can reduce the storage of GL-3 in cultured fibroblasts derived from Fabry patients with amenable mutant forms of α-Gal A.[23–26] As such, AT1001 is currently in clinical development for the evaluation of its safety and efficacy as a monotherapy for Fabry disease in patients with amenable genotypes.[27,28]

The effects of PCs on endogenous wild-type lysosomal enzymes have also been described. For example, isofagomine, a PC for the enzyme deficient in Gaucher disease known as glucocerebrosidase (GCase), increases cellular GCase levels in healthy human volunteers,[18] and improves lysosomal targeting of GCase in cultured normal human fibroblasts.[29] Isofagomine also increases GCase levels in tissues, as well as the central nervous system, of wild-type mice.[29] Similarly, incubation of cultured lymphoblasts or fibroblasts derived from healthy human volunteers with AT1001, or oral administration of AT1001 to healthy human volunteers, results in elevated cellular wild-type α-Gal A levels.[23,30] PCs have also shown beneficial effects on several exogenous recombinant enzymes that are used to treat lysosomal storage disorders. For instance, isofagomine stabilizes recombinant human GCase, protecting it from thermal and pH-mediated denaturation *in vitro*, and can increase uptake of functional enzyme into cultured cells.[31] Similarly, the PCs deoxynojirimycin (DNJ) and *N*-butyl-DNJ can stabilize recombinant human acid α-glucosidase, which is used to treat Pompe disease.[32,33] *In vivo*, oral coadministration of DNJ increases the circulating half-life of intravenously administered recombinant human acid α-glucosidase in rodents and leads to significantly greater enzyme levels and substrate reduction in disease-relevant tissues, namely skeletal, smooth, and cardiac muscle, of Pompe mice.[33] Coadministration of *N*-butyl-DNJ also resulted in greater recombinant human acid α-glucosidase levels in the muscles of Pompe mice.[32] Finally, it was shown recently that AT1001 can slow the denaturation and loss in activity of α-Gal A ERT at neutral pH and body temperature *in vitro*[34] and can increase uptake into cultured Fabry patient-derived cells.[32,34] Most importantly, oral coadministration of AT1001 increases the circulating

levels of active α-Gal A ERT in rodents and humans,[34,35] results in higher tissue α-Gal A levels in mice and Fabry patients,[34,35] and leads to greater GL-3 reduction in disease-relevant tissues of Fabry mice compared to administration of α-Gal A ERT alone.[34] These data point to the potentially beneficial effects of PC coadministration with manufactured ERTs.

In the current study the authors explored an alternative strategy for using AT1001 in combination with a proprietary recombinant human α-Gal A, called ATB100 (manufactured by JCR Pharmaceuticals, Kobe, Hyogo, Japan), where the two were "premixed" into a single formulation for intravenous administration, an approach termed "coformulation". Similar to the published findings with marketed α-Gal A ERT,[34] AT1001 physically stabilizes ATB100 *in vitro* and leads to increased cellular levels of ATB100 in cultured fibroblasts derived from Fabry patients. Intravenous administration of coformulated AT1001 and ATB100 to rodents resulted in a substantially improved pharmacokinetic profile and better tissue targeting and delivery of ATB100. Most importantly, the AT1001-mediated increases in tissue levels of ATB100 resulted in greater GL-3 reduction in Fabry mice that lack endogenous α-Gal A compared to administration of ATB100 alone. Overall, these results demonstrate the potential therapeutic benefits to be gained by coformulating an ERT with a PC and suggest that additional clinical investigations may be warranted.

RESULTS

AT1001 increases the physical stability of ATB100, and prevents aggregation

AT1001 binds ATB100 with high affinity, with an IC_{50} value of 27 nmol/l at pH 7.0, and 29 nmol/l at acidic pH 5.2 (data not shown), similar to the affinity for binding to agalasidase β (unpublished observations). The effect of AT1001 binding on the physical stability of ATB100 was assessed using a fluorescence-based thermal denaturation assay as described earlier.[34,36] At neutral pH, ATB100 was significantly less stable (melting temperature (T_m) 50 °C) than at acidic pH (T_m 59 °C). Importantly, coincubation with AT1001 at neutral pH resulted in a concentration-dependent stabilization of ATB100, with 10 μmol/l AT1001 shifting the T_m to 54.9 °C, and 100 μmol/l AT1001 shifting the T_m to 59.5 °C, which is similar to the T_m of ATB100 at acidic pH (**Figure 1a**). These observations are similar to those with agalsidase β.[30] The ability of AT1001 to prevent aggregation of ATB100 was also assessed. ATB100 was incubated in the absence or presence of AT1001 (10 mg/ml) at neutral pH for 4 weeks at 40 °C, then analyzed by size exclusion-high performance liquid chromatography. In the absence of AT1001, ATB100 showed the presence of a high molecular weight peak (**Figure 1b**) along with a single homodimeric enzyme peak of ~103 kDa. In contrast, coincubation of ATB100 with AT1001 resulted only in a single homodimeric peak (**Figure 1b**). In addition, ATB100 (50 mg/ml) was incubated in the absence and presence of AT1001 (10 mg/ml) at neutral pH for 4 weeks at 40 °C and visually inspected. Notably, while the ATB100 alone vial revealed a white, turbid solution (indicative of aggregation and consistent with the size exclusion-high performance liquid chromatography data), AT1001 coincubation with ATB100 resulted in a clear solution (**Figure 1b, inset**). Collectively, these data indicate that AT1001 can increase the physical stability of exogenous α-Gal
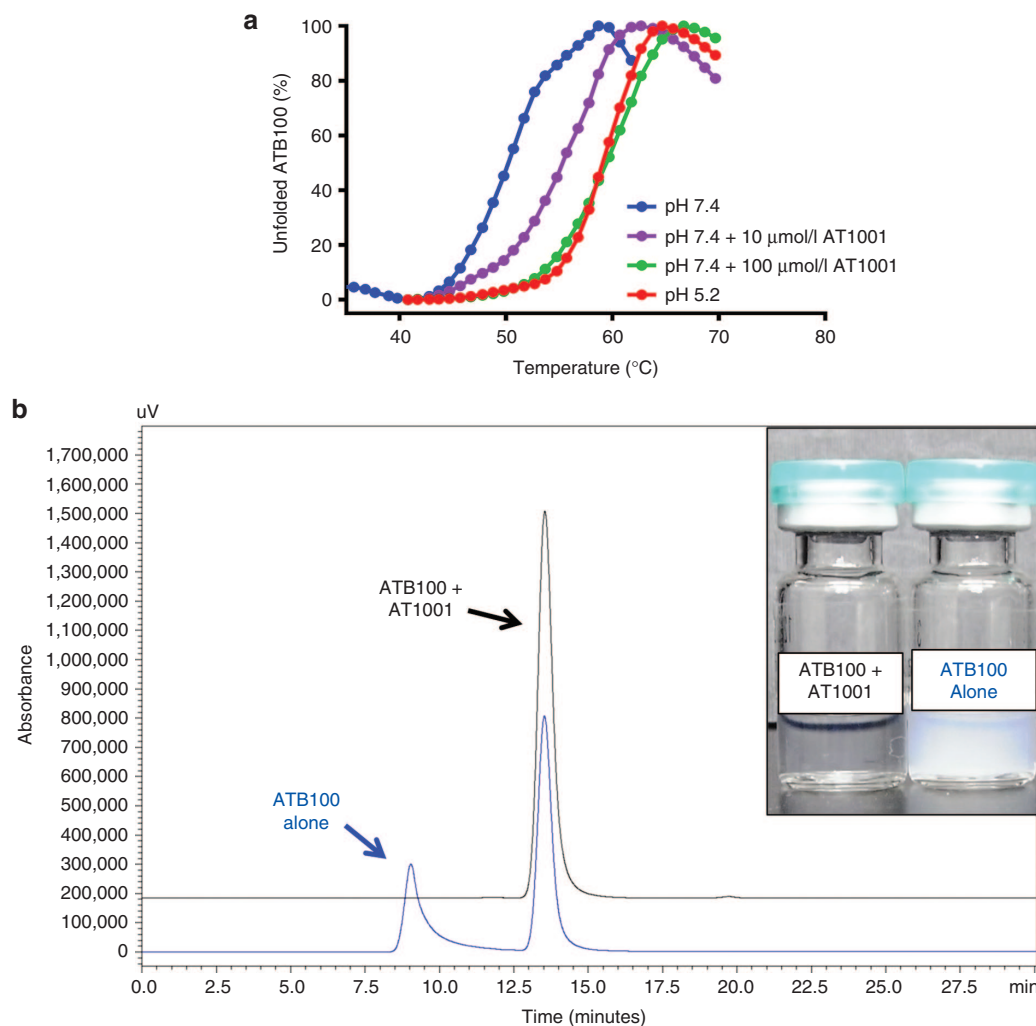
Figure 1 **AT1001 increases the physical stability of ATB100 *in vitro*.** (**a**) Thermal stability scans of ATB100 in the absence and presence of AT1001. Unfolding and denaturation of ATB100 were monitored by changes in the fluorescence of SYPRO Orange as a function of temperature. The thermal stability scans were performed at pH 7.4 in the absence (blue line) and presence of 10 μmol/l (purple line) and 100 μmol/l (green line) AT1001, and at pH 5.2 in the absence of AT1001 (red line). (**b**) Aggregation of ATB100 in the absence and presence of AT1001 at neutral pH for 4 weeks at 40 °C. Size exclusion-high performance liquid chromatography chromatograms showed a single homodimeric enzyme peak with 5 mg/ml ATB100 coincubated with 10 mg/ml AT1001 (black line), but a high molecular weight peak (indicative of aggregate) along with enzyme peak with ATB100 alone (blue line). *Inset*: Aggregation of ATB100 as monitored visually at neutral pH for 4 weeks at 40 °C. The vial of 50 mg/ml ATB100 alone showed clear aggregation as depicted by white turbid solution, whereas the vial coincubated with 10 mg/ml AT1001 resulted in a clear solution. AT, Amicus Therapeutics; ATB, Amicus Therapeutics Biologics.

A ERT, including ATB100, in the neutral pH environment of the blood, protecting the enzyme from irreversible unfolding, denaturation, and aggregation, thereby maintaining the enzyme in a longer-lived, active form.

Coincubation of ATB100 with AT1001 results in greater α-Gal A activity and GL-3 reduction in cultured Fabry fibroblasts compared to incubation with ATB100 alone

The effects of AT1001 coincubation on the cellular levels of ATB100 were assessed in cultured male Fabry patient-derived fibroblast cell lines.[34] Fabry fibroblasts expressing a C52S variant of α-Gal A have no endogenous α-Gal A activity and show no increase in α-Gal A levels in response to incubation with AT1001 alone.[23] Following a 5-hour coincubation of the cells with ATB100 (0.5 nmol/l) and increasing concentrations of AT1001

(0.1–100 μmol/l), cellular α-Gal A activity was up to fourfold higher than the activity measured in cells incubated with ATB100 alone (**Figure 2a** and **Table 1**). Under the same coincubation conditions, cellular GL-3 levels were reduced by up to 45% when measured 10 days postincubation, when compared with a 20% reduction following incubation with ATB100 alone (**Figure 2a**). The coincubation effect on cellular α-Gal A activity and GL-3 levels was dependent on the concentration of AT1001 (**Figure 2a** and **Table 1**). The concentration of ATB100 that yielded 50% of the maximal effect (EC_{50} value) for increased α-Gal A activity was 2.1-fold lower in the presence of AT1001 when compared with incubation with ATB100 alone (**Figure 2b**). Similarly, the EC_{50} value for ATB100-mediated GL-3 reduction was ~2.6-fold lower in the presence of AT1001 when compared with incubation with ATB100 alone (**Figure 2b**). Hence, the potency for ATB100 uptake and ATB100-mediated GL-3 reduction was greater in the
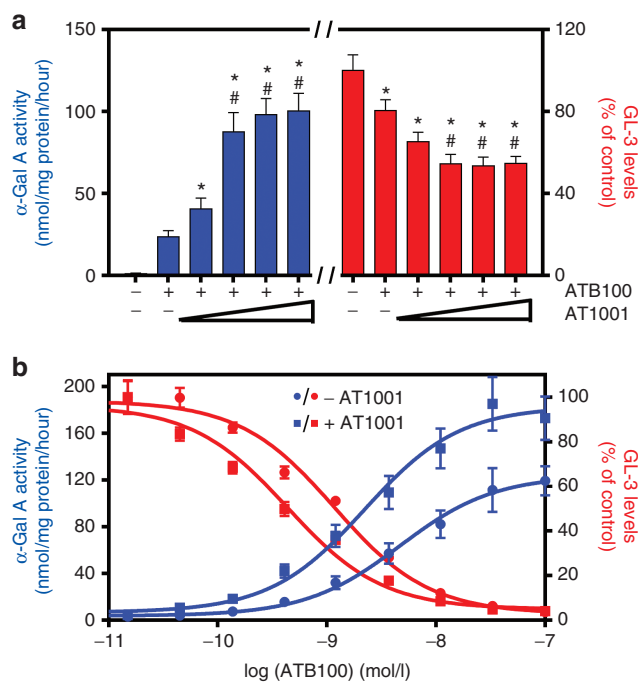
Figure 2 Coincubation of ATB100 with AT1001 enhances cellular α-galactosidase A (α-Gal A) activity and globotriaosylceramide (GL-3) reduction in male Fabry fibroblasts. (a) C52S Fabry fibroblasts were incubated with ATB100 (0.5 nmol/l) alone or in the presence of increasing concentrations of AT1001 (0.1, 1, 10, or 100 µmol/l) for 5 hours. α-Gal A activity (blue bars) and GL-3 levels (red bars) in cell lysates were then measured 2 and 10 days later, respectively. The data points shown are the mean ± SEM of four independent experiments. *$P < 0.05$ compared to baseline; #$P < 0.05$ compared to ATB100 alone, as determined by one-way ANOVA with Bonferroni posthoc analysis. **(b)** C52S Fabry fibroblasts were incubated with increasing concentrations of ATB100 alone or in the presence of 100 µmol/l AT1001 for 5 hours. α-Gal A activity (blue lines) and GL-3 levels (red lines) in cell lysates were measured 2 and 10 days later, respectively. The data points shown are the mean ± SEM of three independent experiments.

Table 1 Effect of coincubation of AT1001 with ATB100 on α-Gal A and GL-3 levels in Fabry patient-derived fibroblasts

| Fibroblast genotype	ATB100 (nmol/l)	AT1001 (µmol/l)	α-Gal A activity (nmol/mg/hour)	GL-3 levels (% control)
C52S (c.155 G>C)	0	0	1 ± 0.5	100 ± 8
	0.5	0	24 ± 4	80 ± 5*
		0.1	41 ± 7*	65 ± 5*
		1.0	88 ± 12*#	55 ± 5*#
		10	98 ± 10*#	53 ± 4*#
		100	100 ± 11*#	54 ± 3*#
R301Q (c.902 G>A)	0	0	3 ± 0.4	100 ± 5
	0.5	0	49 ± 12	73 ± 5*
		0.1	89 ± 20*	65 ± 4*
		1.0	138 ± 21*#	49 ± 6*#
		10	149 ± 25*#	48 ± 6*#
		100	138 ± 19*#	46 ± 8*#

Two male Fabry patient-derived fibroblast cell lines with the indicated genotypes were incubated with ATB100 (0.5 nmol/l) alone or in the presence of increasing concentrations of AT1001 for 5 hours. α-Gal A activity was measured in cell lysates 2 days later. Cellular GL-3 levels (expressed as the percentage of the GL-3 signal measured in untreated Fabry fibroblasts) were measured 10 days later. Data represent the mean ± SEM of three independent experiments. *$P < 0.05$ compared to baseline; #$P < 0.05$ compared to ATB100 incubation alone; one-way ANOVA with Bonferroni posthoc analysis.. α-Gal A, α-galactosidase A; GL-3, globotriaosylceramide.

presence of AT1001. Similar results were seen in a different male Fabry fibroblast cell line that endogenously expresses an AT1001-responsive mutant form of α-Gal A, the R301Q variant (**Table 1**).

AT1001 coformulation increases the circulating half-life and overall exposure of ATB100 in mice

To investigate the *in vivo* effects of ATB100 coformulation with AT1001, the authors first determined the systemic exposure of AT1001 in mice when administered via different routes. Following oral and intravenous (bolus and infusion) administration, AT1001 demonstrated dose-proportional increases in plasma exposure (in both area under the curve (AUC) and C_{max}), with AUCs being similar regardless of the administration route (**Supplementary Table S1**). Next, 1 mg/kg ATB100 was administered alone or coformulated with 3.66 or 12.2 mg/kg AT1001 (equivalent to 3 and 10 mg/kg free base, respectively) via 30-minute intravenous infusion to 8-week-old male C57BL/6 mice. Plasma samples were collected over the following 24-hour period, and α-Gal A activities were measured to determine the systemic exposure of active ATB100. Infusion of ATB100 alone revealed a half-life of ~7 minutes, whereas coformulation with 3.66 or 12.2 mg/kg AT1001 increased the measured half-life to 22 and 34 minutes,

respectively (**Figure 3a, upper panel**). Likewise, the AUC value for ATB100 increased from 17,960 nmol/hour/ml·hour when administered alone to 67,307 and 79,799 nmol/hour/ml·hour when coformulated with 3.66 or 12.2 mg/kg AT1001, respectively (**Figure 3a, upper panel**). These data indicate that coformulation of ATB100 with AT1001 substantially increases the circulating levels of active α-Gal A, with the half-life increasing three- to five-fold, and the AUC increasing 3.8- to 4.4-fold. Similarly, Western blotting revealed greater plasma α-Gal A protein levels following coformulation, supporting the results of the activity measurements (**Figure 3a, lower panel**). A similar study was conducted in 12-week-old male *Gla* KO (knockout) mice, in which a single 30-minute intravenous infusion of 1 or 3 mg/kg ATB100 was given alone or coformulated with 1.22, 3.66, or 12.2 mg/kg AT1001 (equivalent to 1, 3, and 10 mg/kg free base, respectively). Similar to the findings in wild-type C57BL/6 mice, coformulation of ATB100 with AT1001 significantly and dose-dependently increased the circulating levels of active α-Gal A (**Figure 3b**) and α-Gal A protein (data not shown), confirming the positive pharmacokinetic effects of AT1001 coformulation.

Coformulation of ATB100 with AT1001 increases tissue levels and improves biodistribution of α-Gal A in *Gla* KO mice

Twelve-week-old male *Gla* KO mice were given a single 30-minute intravenous infusion of 1 or 3 mg/kg ATB100, either alone or coformulated with 1.22, 3.66, or 12.2 mg/kg AT1001 (equivalent to 1, 3, and 10 mg/kg free base, respectively). Fabry disease-relevant tissues, such as skin, heart, and kidney, were collected 7 days
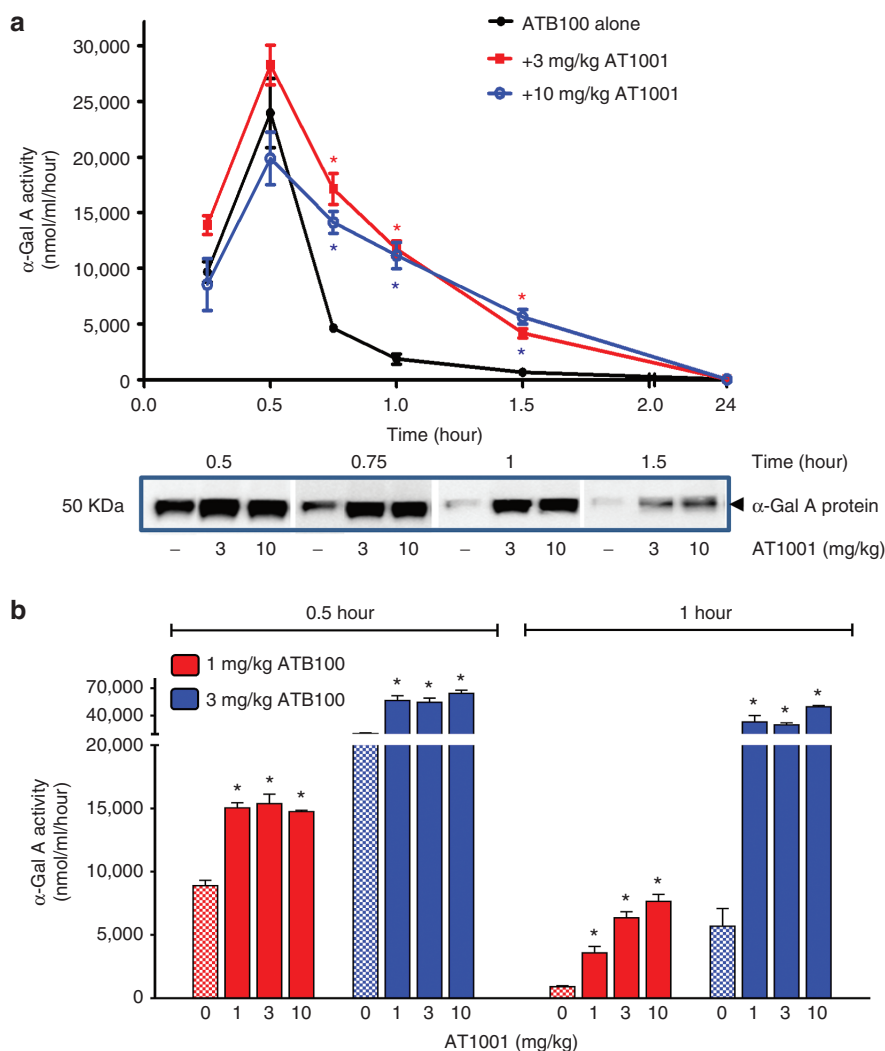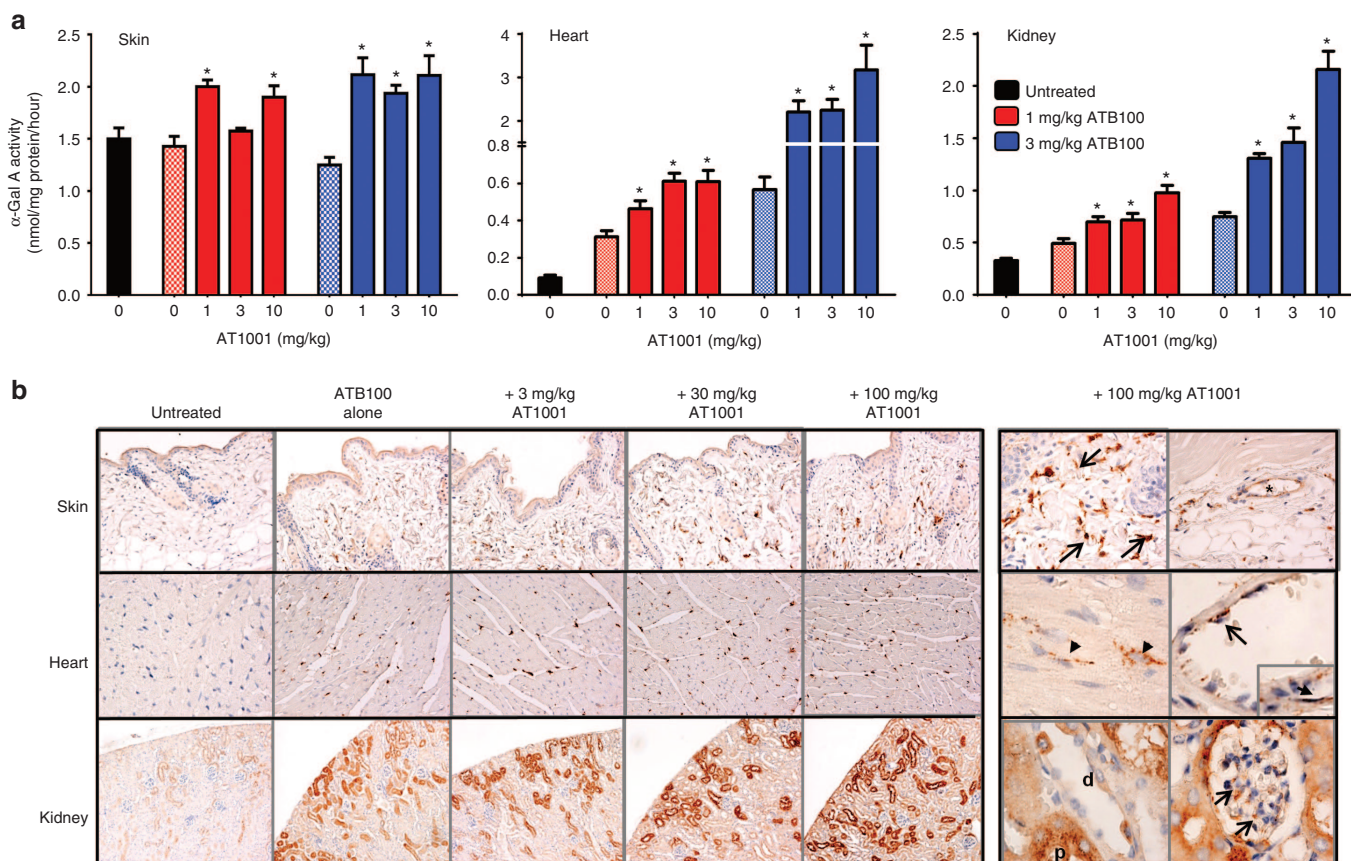
Figure 3 Coformulation of ATB100 with AT1001 increases the total exposure of active ATB100 in mice. (a) Eight-week-old male wild-type C57BL/6 mice were given a single 30-minute intravenous infusion of 1 mg/kg of ATB100, either alone or coformulated with 3.66 or 12.2 mg/kg AT1001 (equivalent to 3 and 10 mg/kg free base, respectively). Plasma samples were collected over the 24-hour period from the start of infusion, and α-galactosidase A (α-Gal A) activity (upper panel) and protein levels (Western blot, lower panel) were measured. For the graph, each time point represents the mean ± SEM of the activity measured from five mice. *$P < 0.05$ compared to ATB100 administration alone; t-test. For the Western blot, each lane contains plasma from a single mouse and is representative of two mice per group. **(b)** Twelve-week-old male *Gla* KO (knockout) mice were given a single 30-minute intravenous infusion of 1 or 3 mg/kg ATB100, either alone or coformulated with 1.22, 3.66, or 12.2 mg/kg AT1001 (equivalent to 1, 3, and 10 mg/kg free base, respectively). Plasma samples were collected via eye bleed 30 minutes and 1 hour after the start of infusion, and α-Gal A activity was determined. Each bar represents the mean ± SEM of the activity measured from five mice per group. *$P < 0.05$ compared to ATB100 administration alone; t-test. Endogenous plasma α-Gal A activity is below the limit of quantitation (7 nmol/ml/hour) in both wild-type and knockout mice.

postinfusion, and tissue levels of ATB100 (measured by α-Gal A activity) were determined. With ATB100 alone, the α-Gal A activity in heart and kidney increased in a dose-dependent manner (**Figure 4a**). With AT1001 coformulation, tissue α-Gal A activity was significantly increased in all three tissues, with up to 2.5-fold higher levels when compared with those seen following administration of ATB100 alone. A modest, apparent dose-dependent effect on α-Gal A activity with AT1001 coformulation was seen in heart and kidney, but not in skin.

Separate studies were conducted to evaluate the effect of coformulation on the biodistribution of ATB100 to disease-relevant cell types. Twelve-week-old male *Gla* KO mice were given a single intravenous bolus injection of 3 mg/kg ATB100, either alone or coformulated with 3.66, 36.6, or 122 mg/kg

AT1001 (equivalent to 3, 30, and 100 mg/kg free base, respectively). Tissues were collected 24 hours postadministration, and immunohistochemical (IHC) staining was performed on paraffin sections using an antihuman α-Gal A antibody (**Figure 4b**). The extent of overall ATB100 uptake was examined initially using ×20 original magnification (left panels). In untreated *Gla* KO mice, no specific α-Gal A IHC signal was detectable in skin (dermis) or heart. With intravenous administration of ATB100 alone, the signals were readily visible, demonstrating ATB100 uptake into these tissues (top left and middle left panels). In kidney, low levels of staining were observed in the proximal tubules of untreated *Gla* KO mice (bottom left). This background was also associated with a number of other commercially available α-Gal A antibodies (data not shown), and was abolished neither by various blocking

Figure 4 Coformulation with AT1001 results in greater tissue levels and biodistribution of ATB100 in *Gla* KO (knockout) mice. (a) Twelve-week-old male *Gla* KO mice were given a single 30-minute intravenous infusion of 1 or 3 mg/kg ATB100, either alone or coformulated with 1.22, 3.66, or 12.2 mg/kg AT1001 (equivalent to 1, 3, and 10 mg/kg free base, respectively). Skin, heart, and kidney were collected 7 days postinfusion, and α-galactosidase A (α-Gal A) activities were determined. Each bar represents the mean ± SEM of five to six mice per group. *$P < 0.05$ compared to ATB100 alone (at the same dose); *t*-test. **(b)** Twelve-week-old male *Gla* KO mice were given an intravenous bolus injection of 3 mg/kg ATB100, either alone or coformulated with 3.66, 36.6, or 122 mg/kg AT1001 (equivalent to 3, 30, and 100 mg/kg free base, respectively). Tissues were collected 24 hours postadministration, and IHC staining was conducted on paraffin sections using an antihuman α-Gal A antibody. Original magnifications of the objective are ×20 (left panels), ×40 (top right panels), or ×100 (middle right and bottom right panels, including the inset). In skin, arrows point to the dermal fibroblasts and the asterisk marks the lumen of a blood vessel (top right). In heart, arrowheads point to cardiomyocytes, whereas cardiac vascular endothelial cells and smooth muscle cells are marked by a large and small arrow (inset), respectively (middle right). In kidney, distal and proximal tubules are labeled as "d" and "p", respectively (bottom left), whereas arrows point to glomerular cells.

or epitope retrieval methods nor by preabsorption of antibody against acetone powder made from untreated *Gla* KO mouse kidney (data not shown), suggesting potential cross-reactivity of the α-Gal A antibody with another protein(s). Nevertheless, IHC signals from ATB100 alone showed a significant increase above the background (bottom left) in kidney. Additional dose-dependent increases in ATB100 uptake were seen in all three tissues with AT1001 coformulation compared to ATB100 alone. Higher magnification (**Figure 4b**, right panels) revealed that AT1001 coformulation resulted in increased ATB100 levels in specific cell types such as dermal fibroblasts (top right, arrows; ×40), dermal blood vessels (top right, asterisk; ×40), cardiomyocytes (middle right, arrowheads; ×100), cardiac vascular endothelial and smooth muscle cells (middle right, large arrow and small arrow in the inset, respectively; ×100), renal distal and proximal tubular epithelial cells (bottom right, d and p, respectively; ×100), and glomerular cells (bottom right, arrows; ×100). Overall, these results indicate that AT1001 coformulation increases the total level of ATB100 in specific disease-relevant cell types.

Coformulation of ATB100 with AT1001 leads to greater substrate reduction in *Gla* KO mice

To determine the effect of AT1001 coformulation on substrate reduction *in vivo*, 14-week-old male *Gla* KO mice were administered ATB100 (0.5, 1, or 3 mg/kg), either alone or coformulated with 1.22, 3.66, or 12.2 mg/kg AT1001 (equivalent to 1, 3, and 10 mg/kg free base, respectively) via intravenous bolus injection (four biweekly administrations). Mice were euthanized 7 days after the final injection, with GL-3 and lyso-Gb$_3$ levels measured in tissues and/or plasma by liquid chromatography in combination with tandem mass spectrometry (LC-MS/MS). Repeat administration of ATB100 alone led to significant, dose-dependent reductions in GL-3 levels in skin, heart, and kidney (**Figure 5**). Furthermore, coformulation of ATB100 with AT1001 generally led to even greater reductions in tissue GL-3 levels when compared with administration of ATB100 alone (**Figure 5**). Of the three doses of AT1001 that were evaluated, 3 mg/kg tended to show the most beneficial effect on ATB100 efficacy. For example, 1 mg/kg ATB100 alone reduced GL-3 levels in skin, heart, and
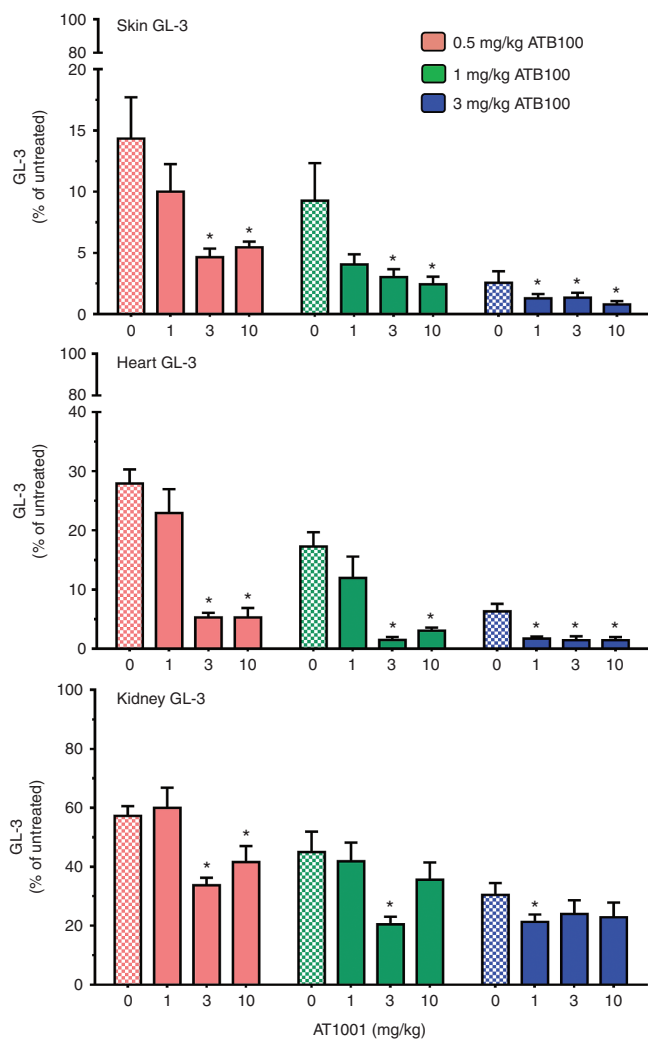
Figure 5 Coformulation of ATB100 with AT1001 leads to greater substrate reduction in *Gla* KO (knockout) mice. Fourteen-week-old male *Gla* KO mice were administered ATB100 (0.5, 1, or 3 mg/kg), either alone or coformulated with 1.22, 3.66, or 12.2 mg/kg AT1001 (equivalent to 1, 3, and 10 mg/kg free base, respectively) via intravenous bolus injection (four biweekly administrations). Plasma and tissues were collected 7 days after the final administration, and globotriaosylceramide (GL-3) levels were measured by liquid chromatography in combination with tandem mass spectrometry. GL-3 levels were normalized to those in untreated *Gla* KO (100%) and wild-type C57BL/6 (0%) mouse tissues (GL-3 levels in *Gla* KO mouse skin, heart, and kidney were 2265, 559, and 778 µg/g tissue, respectively; GL-3 levels in wild-type mouse skin, heart, and kidney were 7, 5, and 75 µg/g tissue, respectively). Each bar represents the mean ± SEM of seven mice per group. *$P < 0.05$ compared to the ATB100 alone (at the same dose); *t*-test.

kidney by ~91%, 83%, and 55%, respectively (green hatched bars, **Figure 5**; **Table 2**). Importantly, when coformulated with 3 mg/kg AT1001, even greater GL-3 reductions of 97%, 98%, and 80%, respectively, were seen (**Figure 5** and **Table 2**). Notably, 1 mg/kg ATB100 alone showed modest effects on kidney GL-3 levels, whereas coformulation with 3 mg/kg AT1001 resulted in ~65% greater reduction. In general, the effect of AT1001 coformulation was more pronounced in the presence of lower ATB100 doses (*e.g.*, 0.5 or 1 mg/kg). Nevertheless, even the highest dose of ATB100 tested in these studies (3 mg/kg), which was very effective

alone and achieved >90% GL-3 reduction in skin and heart, was further improved when coformulated with AT1001, resulting in GL-3 levels that were close to those seen in wild-type mice.

In addition, the GL-3 levels in specific cell types of disease-relevant tissues were assessed qualitatively using IHC methods 7 days after the last ATB100 administration (**Figure 6**) and also were scored based on visual estimation of the number of GL-3-positive cells (see **Supplementary Figure S1**). In skin, IHC revealed two major GL-3 storage sites: fibroblasts and vascular smooth muscle cells (**Figure 6**). The majority of GL-3 accumulated in fibroblasts and was readily reduced by repeat administration of ATB100 alone at the lowest dose (0.5 mg/kg). As a result, the window for further GL-3 reduction on AT1001 coformulation was narrow in fibroblasts. In contrast, dermal vascular smooth muscle cells were less responsive to ATB100 and showed a discernable dose–response with ATB100 alone (**Figure 6** and **Supplementary Figure S1**). In this cell type, further decreases in the GL-3 IHC signals also were observed on coformulation with AT1001 at all three ATB100 dose levels examined. In heart, GL-3 was found mostly in the cardiac vascular smooth muscle cells (**Figure 6**). Like skin, the frequency and intensity of the IHC signals were reduced dose-dependently by administration of ATB100 alone, with a further decrease seen on coformulation with AT1001. In kidney, GL-3 accumulated primarily in distal tubular epithelial cells of the cortex (**Figure 6**). Unlike the tissue GL-3 levels measured by LC-MS/MS, no significant reduction in GL-3 IHC signal was seen in distal tubular epithelial cells following repeat administration of 0.5 mg/kg ATB100 alone (see **Figure 6** and **Supplementary Figure S1**), but the reductions became more pronounced as the dose of ATB100 increased to 3 mg/kg. A further decrease in GL-3 IHC signal was observed on coformulation with AT1001 at all three ATB100 dose levels examined. Overall, these observations are in good agreement with the results from quantitative LC-MS/MS measurements of tissue GL-3, although minor differences can be attributed to tissue handling (paraffin embedding versus tissue lysis), sampling (5 µm section versus tissue lysates), and data acquisition (visual approximation versus quantitative measurement). Consistent with the LC-MS/MS data shown in **Figure 5**, coformulation of AT1001 with 0.5 or 1 mg/kg ATB100 achieved similar or greater GL-3 reduction in all three tissues when compared with the effect at the next higher dose of ATB100 alone (1 and 3 mg/kg, respectively), with the greatest GL-3 reduction attained when 3 mg/kg ATB100 was coformulated with AT1001. Overall, these IHC data indicate a dose-dependent and cell type-specific reduction in GL-3 levels in disease-relevant tissues following repeat administration of ATB100 alone, and profoundly greater reduction of the storage material with AT1001 coformulation.

Finally, the authors evaluated the effect of AT1001 coformulation on the ability of ATB100 to reduce plasma GL-3 and lyso-Gb$_3$. Similar to tissue substrate, dose-dependent reductions in plasma GL-3 were seen. Although 0.5, 1, and 3 mg/kg ATB100 effectively reduced plasma GL-3 levels by 79%, 86%, and 92%, respectively, AT1001 coformulation resulted in maximal GL-3 reductions of ~89%, 91%, and 93%, respectively (**Figure 7a**). Importantly, the effect of AT1001 coformulation on the clinically relevant biomarker plasma lyso-Gb$_3$ was also evaluated. Dose-dependent reductions of 57%, 76%, and 92% were seen in lyso-Gb$_3$ levels with

Table 2 Effect of coformulation of ATB100 with AT1001 on tissue GL-3 levels in *Gla* KO mice

	GL-3 (% reduction)								
Tissue	Skin			Heart			Kidney		
ATB100 (mg/kg)	0.5	1	3	0.5	1	3	0.5	1	3
No AT1001	86 ± 3	91 ± 3	97 ± 1	72 ± 2	83 ± 2	94 ± 1	43 ± 3	55 ± 7	69 ± 4
+1 mg/kg AT1001	90 ± 2	96 ± 1	99 ± 1*	77 ± 4	88 ± 4	98 ± 1*	40 ± 7	58 ± 6	79 ± 2*
+3 mg/kg AT1001	95 ± 1*	97 ± 1*	99 ± 1*	95 ± 1*	98 ± 1*	99 ± 1*	66 ± 2*	80 ± 3*	76 ± 5
+10 mg/kg AT1001	95 ± 1*	98 ± 1*	99 ± 1*	95 ± 2*	97 ± 1*	99 ± 1*	58 ± 5*	64 ± 6	77 ± 5

Fourteen-week-old male *Gla* KO (knockout) mice were administered ATB100 biweekly via bolus tail vein injection with and without AT1001 coformulation for 8 weeks (four injections). Mice were sacrificed 7 days after the fourth ATB100 administration, and tissue GL-3 levels levels were measured as described earlier.[24,34] GL-3 levels were normalized to baseline levels in *Gla* KO (100%) and wild-type C57BL/6 mice (0%). The data presented represent the mean ± SEM for six to seven mice per group.
*$P < 0.05$ compared to ATB100 alone, as determined by unpaired *t*-test. GL-3 levels in *Gla* KO mouse skin, heart, and kidney were 2265, 559, and 778 μg/g tissue, respectively; GL-3 levels in wild-type mouse skin, heart, and kidney were 7, 5, and 75 μg/g tissue, respectively. GL-3, globotriaosylceramide.

0.5, 1, and 3 mg/kg ATB100 alone, respectively (**Figure 7b**). These reductions were further improved with AT1001 coformulation, leading to maximal reductions of ~89%, 92%, and 93%, respectively (**Figure 7b**). Plasma GL-3 and lyso-Gb$_3$ levels showed a significant correlation ($r = 0.9441$, $P < 0.0001$, number of XY pairs = 12, **Figure 7c**). Notably, a very strong correlation was observed between plasma lyso-Gb$_3$ levels and kidney GL-3 levels (nonparametric Spearman correlation $r = 0.9580$, $P < 0.0001$; **Figure 7d**). Good correlations were also observed between plasma lyso-Gb$_3$ levels and heart and skin GL-3 levels ($r = 0.8687$, $P = 0.0005$, and $r = 0.8392$, $P = 0.0011$, respectively; **Figure 7d**).

DISCUSSION

The authors and others have shown earlier that the PC AT1001 can improve the properties of the ERT used to treat Fabry disease.[34,37] These early studies highlighted the ability of the PC to increase the physical stability of Fabry ERT *in vitro* and *ex vivo* (in blood), as well as to substantially enhance the plasma exposure of active enzyme *in vivo* when administered orally prior to ERT infusion. The effects translated to higher cellular and tissue levels of active enzyme, as well as greater substrate reduction *in vitro* and *in vivo*. The earlier studies utilized a "coadministration" approach, whereby AT1001 was administered orally just prior to ERT infusion.[34] These compelling preclinical findings led to the initiation of a clinical study in Fabry patients that also demonstrated greater plasma exposure and greater tissue (skin) levels of active enzyme (for both agalsidase α and agalsidase β) when AT1001 was orally coadministered 2 hours prior to ERT infusion.[35,38]

In the current study, the authors investigated an alternative to coadministration: *i.e.*, *coformulation* of the ERT with the PC, followed by intravenous infusion of the two combined entities. With this approach, a novel, proprietary rhα-Gal A enzyme (ATB100), which is under clinical development by a Japanese group (JCR Pharmaceuticals) was used in combination with AT1001. Previous published literature on rhα-Gal A (agalsidase β) showed less stability at neutral pH (T_m 50 °C)[34] similar to that seen with ATB100. In addition, both enzymes showed ~10 °C shift with AT1001 incubation indicating the two enzymes have similar physical stability.[34]

The coformulation of ATB100 with AT1001 strategy described in the current study allows the PC to bind to the ERT in the formulation, leading to enhanced ERT stabilization even prior to the intravenous delivery, and to potentially similar therapeutic benefit compared to coadministration. Indeed, our preclinical data suggest that coformulation leads to greater exposure of active enzyme in blood, higher cellular and tissue levels of active enzyme after infusion, and greater substrate reduction. This is not surprising given that the overall systemic exposure of AT1001 following intravenous administration to mice is quite similar to that seen in mice orally administered AT1001, especially with respect to AUC. The AUCs following 30-minute intravenous infusion of 3 or 10 mg/kg AT1001 to mice were ~1,909 ng·hour/ml (12 μmol*hour/l) and 6,525 ng·hour/ml (40 μmol*hour/l), respectively, very similar to those achieved following oral gavage: 1,480 ng·hour/ml (9 μmol*hour/l) and 4,520 ng·hour/ml (28 μmol*hour/l), respectively. In humans, comparable AUCs also were achieved following intravenous administration of 0.3 and 1 mg/kg AT1001 (2,283 ng·hour/ml (14 μmol*hour/l) and 6,868 ng·hour/ml (42 μmol*hour/l), respectively),[39] suggesting that similar beneficial pharmacokinetic effects on ERT might be seen in patients at these AT1001 exposures. Interestingly, in Fabry patients, *oral* administration of 150 and 450 mg AT1001 led to AUC values of 13,105 ng/hour/ml (80 μmol*hour/l) and 31,847 n/hour/ml (195 μmol*hour/l), respectively, and resulted in greater α-Gal A activity in plasma and skin when coadministered with ERT.[30,35] Importantly, these exposures are much higher than those seen in mice at doses that lead to beneficial effects on α-Gal A and GL-3 levels and suggest that lower clinical doses, in a coformulation paradigm, might reveal similar benefit.

The proposed mechanism by which coformulation improves the pharmacological properties of ERT is identical to that postulated for coadministration: the PC binds to the exogenous enzyme and increases its physical stability in the blood, protecting it from denaturation and inactivation.[34] This concomitantly increases the likelihood that the ERT is recognized and bound by cell-surface mannose 6-phosphate receptors that are responsible for endocytosis and lysosomal delivery of proteins that contain mannose 6-phosphate, the core determinant for efficient uptake of many ERTs including agalsidase α and β.[40–41] Sufficient uptake is key to the treatment of Fabry disease, as disease-relevant cell types that show greater ERT uptake tend to show better response (*i.e.*, substrate reduction).[8,42–48] Our *in vitro* and *in vivo* coformulation studies support significantly greater cellular and tissue levels of ATB100 when compared with ERT alone. Importantly, AT1001 coformulation also leads to increased tissue α-Gal A levels that
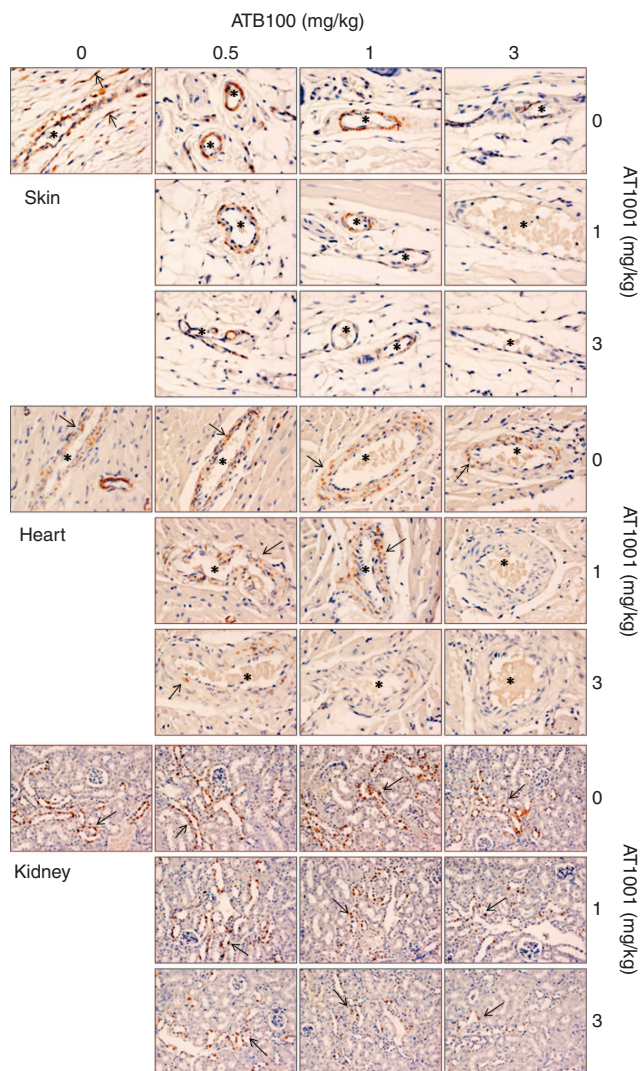
Figure 6 Coformulation of ATB100 with AT1001 enhances cell type-specific globotriaosylceramide (GL-3) reduction in *Gla* KO (knockout) mouse tissues. Fourteen-week-old male *Gla* KO mice were administered ATB1001 (0.5, 1, or 3 mg/kg), either alone or coformulated with 1.22 or 3.66 mg/kg AT1001 (equivalent to 1 and 3 mg/kg free base, respectively) via intravenous bolus injection (four biweekly administrations). Tissues were collected 7 days after the final administration, and GL-3 levels were examined by IHC using an anti-GL-3 antibody. GL-3 signals are shown as brown spots in dermal fibroblasts (arrows) and vascular smooth muscle cells of blood vessels (asterisks), cardiac vascular smooth muscle cells (arrows, with lumens marked by asterisks), and renal distal tubular epithelial cells (arrows). Images were taken with a ×40 objective lens for heart and skin, and a ×20 objective lens for kidney.

are sustained above baseline levels for an extended period of time when compared with administration of ATB100 alone (see **Supplementary Figure S2**). Our IHC results also indicate substantially higher α-Gal A levels in disease-relevant *cell types* of *Gla* KO mice, such as smooth muscle cells of cardiac blood vessels and renal distal tubular epithelial cells, both of which demonstrated concomitant reductions in substrate levels. Notably, the IHC data also show greater α-Gal A levels in cardiomyocytes, cardiac vascular endothelial cells, renal proximal tubular epithelial cells, and glomerular cells, cell types for which substrate reduction could not

be demonstrated in this mouse model because of the lack of GL-3 accumulation. These findings demonstrate that AT1001 coformulation broadly increases the cellular quantity of active ERT, including some cell types that are important for Fabry pathology but which do not demonstrate substantial uptake with ERT alone.

Together with greater cellular and tissue levels of exogenous ERT, our coformulation studies also reveal concomitantly greater GL-3 reduction when compared with ATB100 alone. *In vitro*, coincubation of Fabry patient fibroblasts with ATB100 and AT1001 resulted in ~2.6-fold leftward shift in the EC_{50} value of ATB100 for GL-3 reduction, indicating that AT1001 increases the potency of ATB100. Indeed, AT1001 coincubation with 0.5 nmol/l ATB100 resulted in robust GL-3 reduction that was similar to the maximum reduction observed following incubation with higher concentrations of ATB100 alone (*i.e.*, 5–50 nmol/l). Increased potency of ATB100 was also observed in *Gla* KO mice following coformulation with AT1001. This was most evident for the GL-3 reduction seen at the lower two doses of ATB100 tested (*i.e.*, 0.5 and 1 mg/kg): when coformulated with AT1001, the magnitude of GL-3 reduction was similar to that seen at higher doses of ATB100 alone (*i.e.*, 1 and 3 mg/kg, respectively) in skin, heart, and kidney. These data suggest that AT1001 coformulation with ATB100 can attain the same level of efficacy as seen with higher doses of ATB100 alone.

In our studies, ATB100 coformulation with AT1001 led to greater lyso-Gb_3 reduction in the plasma of *Gla* KO mice when compared with administration of ATB100 alone. Similar to the effects on GL-3, AT1001 coformulation with lower doses of ATB100 (*i.e.*, 0.5 or 1 mg/kg) achieved lyso-Gb_3 reductions that were comparable with, or greater than, those achieved with higher doses of ATB100 alone (*i.e.*, 1 or 3 mg/kg, respectively), indicating that AT1001 also improves the potency of ATB100-mediated reduction of plasma lyso-Gb_3. Interestingly, very strong correlations were observed between plasma lyso-Gb_3 levels and tissue GL-3 levels. It is interesting to note that similar correlations between plasma lyso-Gb_3 levels and kidney interstitial GL-3 levels were seen in Fabry patients in phase 3 studies conducted by Amicus Therapeutics (NCT00925301).[49] Therefore, plasma lyso-Gb_3 could potentially serve as a clinical biomarker to assess long-term treatment outcomes of novel therapeutics in Fabry patients, possibly eliminating the need for invasive procedures to measure substrate levels in tissue biopsies.

In comparison to coadministration, coformulation may offer several additional advantages: first, coformulation of AT1001 with ATB100 allows the chaperone to bind and stabilize the enzyme in the formulation prior to the complex entering the circulation. Thus, coformulation may further minimize the susceptibility of ERT to pH-, temperature-, and/or protease-mediated denaturation/degradation before, during, and after infusion. With coadministration, the chaperone and the ERT enter the circulation independently, with the chaperone binding and stabilizing the enzyme when sufficient concentrations are achieved in the blood. In addition, due to the improved binding efficiency, lower doses of chaperone are sufficient with coformulation compared to coadministration to achieve similar enhancement on the efficacy of ERT. Second, enhanced stability of ATB100 reduces its aggregation/denaturation, which are believed to be key mediators of
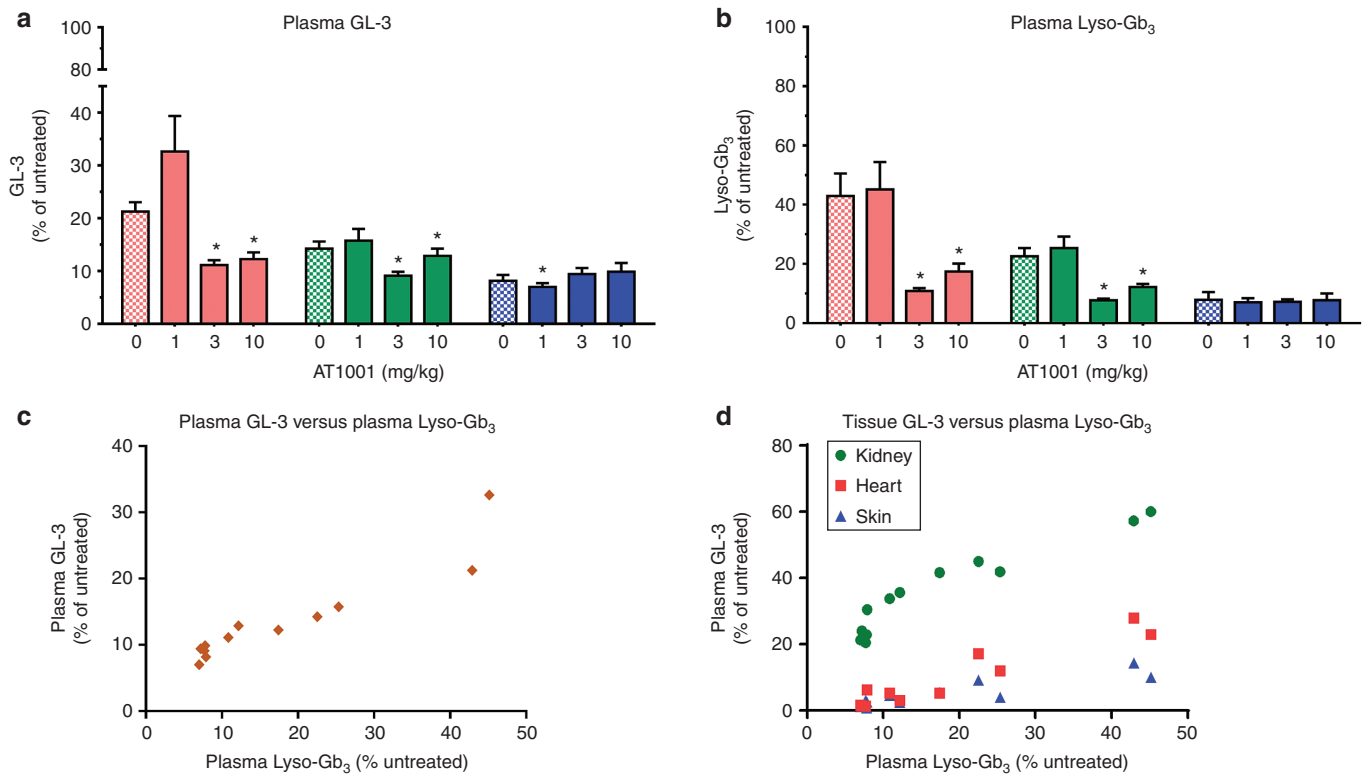
Figure 7 Coformulation of ATB100 with AT1001 leads to greater plasma globotriaosylceramide (GL-3) and globotriaosylsphingosine (lyso-Gb$_3$) reductions in *Gla* KO (knockout) mice. Fourteen-week-old male *Gla* KO mice were administered ATB100 (0.5, 1, or 3 mg/kg), either alone or coformulated with 1.22, 3.66, or 12.2 mg/kg AT1001 (equivalent to 1, 3, and 10 mg/kg free base, respectively) via intravenous bolus injection (four biweekly administrations). Plasma samples were collected 7 days after the final administration, and substrate levels: GL-3 (**a**) and lyso-Gb$_3$ (**b**) were measured by liquid chromatography in combination with tandem mass spectrometry. Substrate levels were normalized to those in *Gla* KO mouse plasma (5 μg/ml and 246 ng/ml, respectively). Each bar represents the mean ± SEM of seven mice per group. *P <0.05 compared to the ATB100 alone (at the same dose); t test. (**c**) Correlation between plasma GL-3 and lyso-Gb$_3$ in mice. (**d**) Correlation between plasma lyso-Gb$_3$ and tissue GL-3 levels in mice.

immunogenicity for various therapeutic proteins as highlighted in many published papers over the last decade. Our data suggest (**Figure 1b**) that coformulation with AT1001 reduces aggregation and thus may reduce infusion-associated reactions and/or immune responses compared to administration of ATB100 alone, which may provide long-term benefits on immunogenicity, an area to explore in future clinical trials. Third, coformulation followed by intravenous administration provide tighter, more precise control of dose and timing, thereby eliminating the dependency on oral bioavailability of the chaperone (many small molecules have poor oral bioavailability) and removing potential pharmacokinetic challenges associated with the effect of food on systemic exposure (*i.e.*, the absorption of AT1001 is substantially slower and less predictable in the fed state compared to the fasted state, as is the case with many other small molecule drugs).

AT1001 coformulation with ERT is believed to be broadly applicable to the diverse Fabry patient population, and is independent of patient genotype. The majority of beneficial effects of coformulation was demonstrated in cell- and mouse-based models that are deficient in α-Gal A activity and protein, indicating that the efficacy of coformulation is mediated largely through AT1001 stabilizing the exogenous ERT. This is an important distinction from AT1001 monotherapy, where the positive therapeutic effect is dictated by patient genotype and the ability of AT1001 to bind and stabilize the endogenous, mutant form of α-Gal A in

the ER, thereby leading to enhanced lysosomal trafficking and substrate reduction.[23–24,50–51] In this case, AT1001 is administered alone and with a more frequent interval (*e.g.*, every other day, as opposed to every other week in the coformulation paradigm). Amicus Therapeutics has recently completed two phase 3 studies with AT1001 monotherapy in Fabry subjects (NCT00925301; NCT01218659), with clinical efficacy currently under evaluation. Thus, for patients with amenable mutant forms of endogenous α-Gal A, AT1001 monotherapy may become a therapeutic option; the coformulation of AT1001 with ERT, on the other hand, could be applicable to the broad Fabry population, regardless of patient genotype.

Overall, our data indicate that AT1001 coformulation stabilizes the novel, proprietary Fabry ERT ATB100 in a long-lived, active conformation in the circulation, thereby leading to delivery of higher levels of active enzyme to disease-relevant cells and tissues, and translating to subsequently greater substrate reduction *in situ*, potentially in cell types that typically do not respond well to currently marketed ERTs. Similar to the coadministration paradigm, the potentially beneficial effects of coformulating a PC with a Fabry ERT into a single product that can be administered via the intravenous route also may warrant clinical investigation and, if successful, could serve as a next-generation approach to ERT in Fabry patients. As such, this work also has broad implications for the existing and future ERTs across multiple lysosomal storage disorders, as well as

protein therapeutics in general, as it provides a novel and potentially better therapeutic strategy that allows the chaperone to bind and stabilize the therapeutic protein in the formulation prior to administration, providing enhanced activity for an extended duration *in vivo* and perhaps fewer tolerability issues overall.

MATERIALS AND METHODS

Materials. Male Fabry patient-derived fibroblasts (C52S, c.155 G>C; R301Q, c.902 G>A) were from sources described earlier.[23] All cell culture reagents were purchased from Invitrogen (Carlsbad, CA), except for characterized fetal bovine serum (HyClone, Waltham, MA). AT1001 (1-deoxygalactonojirimycin hydrochloride; migalastat hydrochloride) was synthesized by Cambridge Major Laboratories (Germantown, WI). ATB100 (recombinant human α-Gal A, JR-051) was a kind gift from JCR Pharmaceuticals. Mouse antihuman GL-3 monoclonal antibody was purchased from Seikagaku Corporation (Tokyo, Japan). Rabbit antihuman α-Gal A antibody was purchased from Sigma–Aldrich (St Louis, MO). Horseradish peroxidase-conjugated goat antirabbit secondary antibody was purchased from ThermoPierce (Rockford, IL). *Gla* KO mice were obtained from Robert Desnick (Mount Sinai University, New York, NY). Wild-type C57BL/6 mice were purchased from Taconic Farms (Germantown, NY). Animal husbandry and all experiments were conducted under Institutional Animal Care and Use Committee approved protocols of Rutgers State University. All other reagents were purchased from Sigma–Aldrich unless noted otherwise.

Thermal stability assay. The stability of ATB100 was assessed using a modified fluorescence thermostability assay[34,52] on an Agilent Stratagene Mx3005P system (Eppendorf, Hamburg, Germany) in either neutral pH buffer (25 mmol/l sodium phosphate, 150 mmol/l sodium chloride, pH 7.4) or acidic pH buffer (25 mmol/l sodium acetate, 150 mmol/l sodium chloride, pH 5.2). In brief, ATB100 (3.0 µg) was combined with SYPRO Orange (Life Technologies, Carlsbad, CA) and the indicated concentrations of AT1001 in a final reaction volume of 25 µl. A thermal gradient was applied to the plate at a rate of 1 °C/minute, during which the fluorescence of SYPRO Orange was continuously monitored. The fluorescence intensity at each temperature was normalized to the maximum fluorescence after complete thermal denaturation and analyzed by a Boltzman sigmoidal nonlinear regression to determine the melting temperatures (T_m).

Assay to measure aggregation of ATB100. Aggregation of ATB100 in the absence and presence of AT1001 was measured using size exclusion-high performance liquid chromatography detection. ATB100 (5 mg/ml) was incubated in the absence or presence of AT1001 (10 mg/ml) at neutral pH for 4 weeks at 40 °C. After 4 weeks, samples were run on a silica-based TSKG3000SWXL analytical column (Tosoh, Tokyo, Japan). Nearly 5 µl of ATB100 (concentration adjusted to 5 mg/ml) were loaded onto the column and eluted with phosphate-buffered saline solution (25 mmol/l sodium phosphate, 150 mmol/l NaCl, pH 6.0) at a flow rate of 0.6 ml/minute, with detection at 215 nm. For visual monitoring of aggregation, ATB100 (50 mg/ml) was incubated in the absence or presence of AT1001 (10 mg/ml) at neutral pH for 4 weeks at 40 °C. After 4 weeks, samples were visually inspected for turbidity.

α-Gal A activity assay and immunofluorescence detection of GL-3 in Fabry patient fibroblasts. Cellular levels of ATB100 activity and GL-3 were assessed in Fabry patient fibroblasts as described earlier.[34]

ATB100/AT1001 coformulation studies in wild-type and Gla KO mice. In the study shown in **Figure 3a**, 8-week-old male wild-type C57BL/6 mice were given a single 30-minute intravenous infusion (via jugular vein cannula) of either 1 mg/kg ATB100 alone or 1 mg/kg ATB100 that was coformulated with 3.66 or 12.2 mg/kg AT1001 (equivalent to 3 and 10 mg/kg free base, respectively). For coformulation, the dosing solutions were

prepared by adding saline, followed by AT1001, ATB100 then gentle mixing. The ATB100–AT1001 solution was incubated at room temperature for 30 minutes prior to administration. Blood was collected via eye bleed 15, 30, and 45 minutes, as well as 1, 1.5, and 24 hours after the start of infusion. Plasma was derived by spinning whole blood at 2,700 g for 10 minutes at 4 °C. ATB100 exposure was determined by measuring α-Gal A activity in plasma. In the studies shown in **Figures 3b** and **4a**, 12-week-old male *Gla* KO mice were given a single 30-minute intravenous infusion of 1 or 3 mg/kg ATB100, either alone or coformulated with 1.22, 3.66, or 12.2 mg/kg AT1001 (equivalent to 1, 3, and 10 mg/kg free base, respectively). Blood was collected via eye bleed 30 minutes and 1 hour after the start of infusion, and α-Gal A activity was determined in plasma. In the study shown in **Figure 4b**, 12-week-old male *Gla* KO mice were administered 3 mg/kg ATB100 either alone or coformulated with 3.66, 36.6, or 122 mg/kg AT1001 (equivalent to 3, 30, and 100 mg/kg free base, respectively) via bolus tail vein injection. Mice were euthanized 24 hours after ATB100 administration and tissues were collected for IHC detection of α-Gal A. In the studies shown in **Figures 5** and **6**, 12-week-old male *Gla* KO mice were administered ATB100 (0.5, 1, or 3 mg/kg) either alone or coformulated with 1.22, 3.66, or 12.2 mg/kg AT1001 (equivalent to 1, 3, and 10 mg/kg free base, respectively) via bolus tail vein injection every other week for 8 weeks (total four administrations). In the study shown in **Figure 7**, 12-week-old male *Gla* KO mice were administered ATB100 (3 mg/kg) either alone or coformulated with 3.66 mg/kg AT1001 (equivalent to 3 mg/kg free base, respectively) via bolus tail vein injection every other week for 8 weeks (total four administrations). Mice were euthanized 7 days after the final (fourth) ATB100 administration, and plasma GL-3 and lyso-Gb3 levels were measured using LC-MS/MS as described in what follows.

Analytical methods. From all the aforementioned studies, heart, kidney, and skin (shaved and removed from the lower ventral side of the neck) were quickly removed, rinsed in cold PBS, blotted dry, and stored on dry ice. Tissue and plasma α-Gal A activity, plasma α-Gal A protein (by Westerns), and tissue and plasma GL-3 levels were assessed using methodologies described earlier.[24,34,53] For plasma lyso-Gb$_3$, the method was similar as used earlier[53] with some modifications. In brief, 50 µl of mouse plasma was added to 50 µl of internal standard working solution (75 ng/ml $^{13}C_6$-lyso-Gb$_3$ (synthesized at Amicus, based on the study by Gold *et al.*[54]) in dimethyl sulfoxide:methanol/1:1) and 1.0 ml of MeOH. Five hundred microliters of 1 N HCl were then added, and the samples were shaken for 30–45 minutes (VWR multitube vortexer) and then centrifuged at 3,220 g for 10 minutes. Supernatant was transferred to preconditioned SPE cartridges (Waters, Oasis, MCX, Milford, MA). The SPE cartridges were washed and then eluted with 2.0 ml of 5% NH$_4$OH in MeOH. Samples were then evaporated to dryness at 40 °C under nitrogen gas, reconstituted, and transferred to glass autosampler vials for LC-MS/MS analysis. Liquid chromatography was conducted using a binary mobile phase gradient on a hydrophilic interaction chromatography column (75 × 4.6 mm) with a flow rate of 0.550 ml/minute. MS/MS analysis was carried out under positive electrospray ionization using the lyso-Gb$_3$ and $^{13}C_6$-lyso-Gb$_3$ MRM transitions of 786 > 282 and 792 > 282, respectively. The ratio of the total lyso-Gb$_3$ area counts to that of the internal standard was determined and used to calculate the final concentration of lyso-Gb$_3$ in each plasma sample. The assay range was 0.200–200 ng/ml, based on a linear least squares fit equation calibration curve ($1/x^2$ weighting) prepared in DMSO:MeOH/1:1.

Immunohistochemistry. Samples of skin, heart, and kidney were stored in Z-Fix (Anatech, Battle Creek, MI) and processed into paraffin. Sections were cut at a 5-µm thickness. The IHC detection of GL-3 was conducted as described earlier.[24] The IHC detection of ATB100 in tissues was conducted using a rabbit antihuman α-Gal A antibody (HPA000237, 1:1,000 dilution; Sigma), coupled with rabbit-on-rodent HRP polymer (Biocare Medical, Concord, CA), and developed with DAB betazoid chromogen (Biocare Medical). Heat-induced epitope retrieval was carried out in 0.1 M Tris–5% urea solution (pH 9.5) prior to the addition of the anti-α-Gal A antibody.

Data analysis. Determinations of statistical significance were conducted using Excel 2003 (Microsoft, Redmond, WA) or GraphPad Prism, version 6 (Graph Pad Software, San Diego, CA) as defined in the figure and table legends. Linear trends for dose-dependence were calculated using a one-way ANOVA in GraphPad Prism. The half-life ($t_{1/2}$) of ATB100 in plasma was calculated using a nonlinear, one-phase exponential decay curve fitting function in GraphPad Prism. Analysis of the pharmacokinetic profile of AT1001 was conducted using noncompartmental analysis using Phoenix WinNonLin, Version 6.1. For correlations of plasma GL-3 and plasma lyso-Gb$_3$, substrate levels were normalized to the levels in untreated *Gla* KO mouse plasma (5 μg/mL and 246 ng/ml, respectively). For correlations of tissue GL-3 and plasma lyso-Gb$_3$, tissue GL-3 levels were normalized to the levels in untreated *Gla* KO mouse tissues after subtracting wild-type levels (GL-3 levels in *Gla* KO mouse skin, heart, and kidney are 2,265, 559, and 778 μg/g tissue, respectively; wild-type GL-3 levels in skin, heart, and kidney are 7, 5, and 75 μg/g tissue, respectively). The mean values of each treatment group were analyzed for nonparametric Spearman correlation.

SUPPLEMENTARY MATERIAL

Figure S1. Semi-quantitative assessment of tissue GL-3 levels using a visual scoring method after IHC staining.
Figure S2. AT1001 coformulation shows longer sustained tissue α-Gal A levels compared to ATB100 alone.
Table S1. Systemic exposure of AT1001 in mice following various routes of administration.

REFERENCES

1. Brady, RO, Gal, AE, Bradley, RM, Martensson, E, Warshaw, AL and Laster, L (1967). Enzymatic defect in Fabry's disease. Ceramidetrihexosidase deficiency. *N Engl J Med* **276**: 1163–1167.
2. Desnick, R, Ioannou, Y and Eng, C (2001). α-galactosidase A deficiency: Fabry disease. In: *The Metabolic and Molecular Bases of Inherited Disease*. McGraw-Hill: New York. pp. 3733–3774.
3. Askari, H, Kaneski, CR, Semino-Mora, C, Desai, P, Ang, A, Kleiner, DE et al. (2007). Cellular and tissue localization of globotriaosylceramide in Fabry disease. *Virchows Arch* **451**: 823–834.
4. Aerts, JM, Groener, JE, Kuiper, S, Donker-Koopman, WE, Strijland, A, Ottenhoff, R et al. (2008). Elevated globotriaosylsphingosine is a hallmark of Fabry disease. *Proc Natl Acad Sci USA* **105**: 2812–2817.
5. Rombach, SM, Dekker, N, Bouwman, MG, Linthorst, GE, Zwinderman, AH, Wijburg, FA et al. (2010). Plasma globotriaosylsphingosine: diagnostic value and relation to clinical manifestations of Fabry disease. *Biochim Biophys Acta* **1802**: 741–748.
6. Togawa, T, Kodama, T, Suzuki, T, Sugawara, K, Tsukimura, T, Ohashi, T et al. (2010). Plasma globotriaosylsphingosine as a biomarker of Fabry disease. *Mol Genet Metab* **100**: 257–261.
7. Togawa, T, Kawashima, I, Kodama, T, Tsukimura, T, Suzuki, T, Fukushige, T et al. (2010). Tissue and plasma globotriaosylsphingosine could be a biomarker for assessing enzyme replacement therapy for Fabry disease. *Biochem Biophys Res Commun* **399**: 716–720.
8. Eng, CM, Banikazemi, M, Gordon, RE, Goldman, M, Phelps, R, Kim, L et al. (2001). A phase ½ clinical trial of enzyme replacement in Fabry disease: pharmacokinetic, substrate clearance, and safety studies. *Am J Hum Genet* **68**: 711–722.
9. Schiffmann, R, Kopp, JB, Austin, HA 3rd, Sabnis, S, Moore, DF, Weibel, T et al. (2001). Enzyme replacement therapy in Fabry disease: a randomized controlled trial. *JAMA* **285**: 2743–2749.
10. Hughes, DA, Elliott, PM, Shah, J, Zuckerman, J, Coghlan, G, Brookes, J et al. (2008). Effects of enzyme replacement therapy on the cardiomyopathy of Anderson–Fabry disease: a randomised, double-blind, placebo-controlled clinical trial of agalsidase alfa. *Heart* **94**: 153–158.
11. Schiffmann, R, Germain, DP, Castelli, J, Shenker, A and Lockhart, DJ (2008). 768/T. *Phase 2 clinical trials of the pharmacological chaperone AT1001 for the treatment of Fabry disease.* Presented at the American Society of Human Genetics Conference, Philadelphia, 11–15 November 2008.
12. West, M, Nicholls, K, Mehta, A, Clarke, JT, Steiner, R, Beck, M et al. (2009). Agalsidase alfa and kidney dysfunction in Fabry disease. *J Am Soc Nephrol* **20**: 1132–1139.
13. Thurberg, BL, Rennke, H, Colvin, RB, Dikman, S, Gordon, RE, Collins, AB et al. (2002). Globotriaosylceramide accumulation in the Fabry kidney is cleared from multiple cell types after enzyme replacement therapy. *Kidney Int* **62**: 1933–1946.
14. Bénichou, B, Goyal, S, Sung, C, Norfleet, AM and O'Brien, F (2009). A retrospective analysis of the potential impact of IgG antibodies to agalsidase beta on efficacy during enzyme replacement therapy for Fabry disease. *Mol Genet Metab* **96**: 4–12.
15. Bodensteiner, D, Scott, CR, Sims, KB, Shepherd, GM, Cintron, RD and Germain, DP (2008). Successful reinstitution of agalsidase beta therapy in Fabry disease patients with previous IgE-antibody or skin-test reactivity to the recombinant enzyme. *Genet Med* **10**: 353–358.
16. Tesmoingt, C, Lidove, O, Reberga, A, Thetis, M, Ackaert, C, Nicaise, P et al. (2009). Enzyme therapy in Fabry disease: severe adverse events associated with anti-agalsidase cross-reactive IgG antibodies. *Br J Clin Pharmacol* **68**: 765–769.
17. Fan, JQ and Ishii, S (2003). Cell-based screening of active-site specific chaperone for the treatment of Fabry disease. *Methods Enzymol* **363**: 412–420.
18. Valenzano, KJ, Khanna, R, Powe, AC, Boyd, R, Lee, G, Flanagan, JJ et al. (2011). Identification and characterization of pharmacological chaperones to correct enzyme deficiencies in lysosomal storage disorders. *Assay Drug Dev Technol* **32**: 213–235.
19. Asano, N, Nash, RJ, Molyneux, RJ and Fleet, GWJ (2000). Sugar-mimic glycosidase inhibitors: natural occurrence, biological activity and prospects for therapeutic application. *Tetrahedron: Asymmetry* **11**: 1645–1680.
20. Shin, SH, Murray, GJ, Kluepfel-Stahl, S, Cooney, AM, Quirk, JM, Schiffmann, R et al. (2007). Screening for pharmacological chaperones in Fabry disease. *Biochem Biophys Res Commun* **359**: 168–173.
21. Fan, JQ, Ishii, S, Asano, N and Suzuki, Y (1999). Accelerated transport and maturation of lysosomal alpha-galactosidase A in Fabry lymphoblasts by an enzyme inhibitor. *Nat Med* **5**: 112–115.
22. Yam, GH, Zuber, C and Roth, J (2005). A synthetic chaperone corrects the trafficking defect and disease phenotype in a protein misfolding disorder. *FASEB J* **19**: 12–18.
23. Benjamin, ER, Flanagan, JJ, Schilling, A, Chang, HH, Agarwal, L, Katz, E et al. (2009). The pharmacological chaperone 1-deoxygalactonojirimycin increases alpha-galactosidase A levels in Fabry patient cell lines. *J Inherit Metab* **32**: 424–440.
24. Khanna, R, Soska, R, Lun, Y, Feng, J, Frascella, M, Young, B et al. (2010). The pharmacological chaperone 1-deoxygalactonojirimycin reduces tissue globotriaosylceramide levels in a mouse model of Fabry disease. *Mol Ther* **18**: 23–33.
25. Yam, GH, Bosshard, N, Zuber, C, Steinmann, B and Roth, J (2006). Pharmacological chaperone corrects lysosomal storage in Fabry disease caused by trafficking-incompetent variants. *Am J Physiol Cell Physiol* **290**: C1076–C1082.
26. Ishii, S, Chang, HH, Yoshioka, H, Shimada, T, Mannen, K, Higuchi, Y et al. (2009). Preclinical efficacy and safety of 1-deoxygalactonojirimycin in mice for Fabry disease. *J Pharmacol Exp Ther* **328**: 723–731.
27. Germain, DP, Giugliani, R, Hughes, DA, Mehta, A, Nicholls, K, Barisoni, L et al. (2012). Safety and pharmacodynamic effects of a pharmacological chaperone on α-galactosidase A activity and globotriaosylceramide clearance in Fabry disease: report from two phase 2 clinical studies. *Orphanet J Rare Dis* **7**: 91.
28. Giugliani, R, Waldek, S, Germain, DP, Nicholls, K, Bichet, DG, Simosky, JK et al. (2013). A Phase 2 study of migalastat hydrochloride in females with Fabry disease: selection of population, safety and pharmacodynamic effects. *Mol Genet Metab* **109**: 86–92.
29. Khanna, R, Benjamin, ER, Pellegrino, L, Schilling, A, Rigat, BA, Soska, R et al. (2010). The pharmacological chaperone isofagomine increases the activity of the Gaucher disease L444P mutant form of beta-glucosidase. *FEBS J* **277**: 1618–1638.
30. Johnson, FK, Mudd, PN, Bragat, A, Adera, M and Boudes, P (2013). Pharmacokinetics and safety of migalastat HCl and effects on agalsidase activity in healthy volunteers. *Clin Pharmacol Drug Dev* **2**: 120–132.
31. Shen, JS, Edwards, NJ, Hong, YB and Murray, GJ (2008). Isofagomine increases lysosomal delivery of exogenous glucocerebrosidase. *Biochem Biophys Res Commun* **369**: 1071–1075.
32. Porto, C, Cardone, M, Fontana, F, Rossi, B, Tuzzi, MR, Tarallo, A et al. (2009). The pharmacological chaperone N-butyldeoxynojirimycin enhances enzyme replacement therapy in Pompe disease fibroblasts. *Mol Ther* **17**: 964–971.
33. Khanna, R, Flanagan, JJ, Feng, J, Soska, R, Frascella, M, Pellegrino, LJ et al. (2012). The pharmacological chaperone AT2220 increases recombinant human acid α-glucosidase uptake and glycogen reduction in a mouse model of Pompe disease. *PLoS One* **7**: e40776.
34. Benjamin, ER, Khanna, R, Schilling, A, Flanagan, JJ, Pellegrino, LJ, Brignol, N et al. (2012). Co-administration with the pharmacological chaperone AT1001 increases recombinant human α-galactosidase A tissue uptake and improves substrate reduction in Fabry mice. *Mol Ther* **20**: 717–726.
35. Warnock, DG, Bichet, DG, Holida, M, Goker-Alpan, O, Nicholls, K, Thomas, M et al. (2015). Oral migalastat HCl leads to greater systemic exposure and tissue levels of active α-galactosidase A in Fabry patients when co-administered with infused agalsidase. *PLoS ONE* (manuscript submitted).
36. Flanagan, JJ, Rossi, B, Tang, K, Wu, X, Mascioli, K, Donaudy, F et al. (2009). The pharmacological chaperone 1-deoxynojirimycin increases the activity and lysosomal trafficking of multiple mutant forms of acid alpha-glucosidase. *Hum Mutat* **30**: 1683–1692.
37. Porto, C, Pisani, A, Rosa, M, Acampora, E, Avolio, V, Tuzzi, MR et al. (2012). Synergy between the pharmacological chaperone 1-deoxygalactonojirimycin and the human recombinant alpha-galactosidase A in cultured fibroblasts from patients with Fabry disease. *J Inherit Metab Dis* **35**: 513–520.
38. Johnson, F, Kishnani, P, Tarnopolsky, M, Sivakumar, K, Byrne, B, Goker-Alpan, O et al. (2012). An ongoing phase 2A study to investigate the effect of AT2220 (duvoglustat HCl) on the pharmacokinetics of acid alpha-glucosidase in subjectswith Pompe disease: preliminary results. *J Inherit Metab Dis* **35**: S96.
39. Hughes, D, Skuban, N, Johnson, F, Lazauskas, R, Williams, H, Kirk, J et al. (2014). Development of a next-generation ERT, ATB100C, for Fabry disease. *J Inherit Metab Dis* **37**: S158.
40. Coutinho, MF, Prata, MJ and Alves, S (2012). Mannose-6-phosphate pathway: a review on its role in lysosomal function and dysfunction. *Mol Genet Metab* **105**: 542–550.

41. Mayes, JS, Cray, EL, Dell, VA, Scheerer, JB and Sifers, RN (1982). Endocytosis of lysosomal alpha-galactosidase A by cultured fibroblasts from patients with Fabry disease. *Am J Hum Genet* **34**: 602–610.

42. Eng, CM, Guffon, N, Wilcox, WR, Germain, DP, Lee, P, Waldek, S *et al.*; International Collaborative Fabry Disease Study Group (2001). Safety and efficacy of recombinant human alpha-galactosidase A—replacement therapy in Fabry's disease. *N Engl J Med* **345**: 9–16.

43. Germain, DP (2010). Fabry disease. *Orphanet J Rare Dis* **5**: 30.

44. Germain, DP, Waldek, S, Banikazemi, M, Bushinsky, DA, Charrow, J, Desnick, RJ *et al.* (2007). Sustained, long-term renal stabilization after 54 months of agalsidase beta therapy in patients with Fabry disease. *J Am Soc Nephrol* **18**: 1547–1557.

45. Keslová-Veselíková, J, Hůlková, H, Dobrovolný, R, Asfaw, B, Poupetová, H, Berná, L *et al.* (2008). Replacement of alpha-galactosidase A in Fabry disease: effect on fibroblast cultures compared with biopsied tissues of treated patients. *Virchows Arch* **452**: 651–665.

46. Schiffmann, R, Rapkiewicz, A, Abu-Asab, M, Ries, M, Askari, H, Tsokos, M *et al.* (2006). Pathological findings in a patient with Fabry disease who died after 2.5 years of enzyme replacement. *Virchows Arch* **448**: 337–343.

47. Thurberg, B, Rennke, H, Colvin, R, Dikman, S, Gordon, R and O'Callaghan, M (2008). Pathology of Fabry nephropathy: renal fibrosis may begin in adolescence. *Mol Genet Metab* **93**: 39–39.

48. Lee, K, Jin, X, Zhang, K, Copertino, L, Andrews, L, Baker-Malcolm, J *et al.* (2003). A biochemical and pharmacological comparison of enzyme replacement therapies for the glycolipid storage disorder Fabry disease. *Glycobiology* **13**: 305–313.

49. Benjamin, E, Hamler, R, Brignol, N, Boyd, R, Yu, J, Bragat, A *et al.* (2014). Migalastat reduces plasma globotriaosylsphingosine (lyso-Gb3) in Fabry patients: results from the facets phase 3 study. *J Inherit Metab Dis* **37**: S161.

50. Wu, X, Katz, E, Della Valle, MC, Mascioli, K, Flanagan, JJ, Castelli, JP *et al.* (2011). A pharmacogenetic approach to identify mutant forms of α-galactosidase A that respond to a pharmacological chaperone for Fabry disease. *Hum Mutat* **32**: 965–977.

51. Wu, X, Della Valle, M, Katz, E, Mascioli, K, Schiffmann, R, Castelli, J *et al.* (2011). A pharmacogenetic approach to identify mutant forms of α-galactosidase A that respond to a pharmacological chaperone for Fabry disease. *J Inherit Metab Dis* **34**: S190.

52. Niesen, FH, Berglund, H and Vedadi, M (2007). The use of differential scanning fluorimetry to detect ligand interactions that promote protein stability. *Nat Protoc* **2**: 2212–2221.

53. Young-Gqamana, B, Brignol, N, Chang, HH, Khanna, R, Soska, R, Fuller, M *et al.* (2013). Migalastat HCl reduces globotriaosylsphingosine (lyso-Gb3) in Fabry transgenic mice and in the plasma of Fabry patients. *PLoS One* **8**: e57631.

54. Gold, H, Boot, RG, Aerts, JMFG, Overkleeft, HS, Codée, JDC and van der Marel, GA (2011). A concise synthesis of globotriaosylsphingosine. *Eur J Org Chem* **2011**: 1652–1663.